NATIONAL AIR INTELLIGENCE CENTER

DTIC
SELECTE
MAY 1 5 1995
S C D

1.06 μm LASER-INDUCED DAMAGE OF TI AND ZR THIN-FILM
OPTICAL COATINGS

by

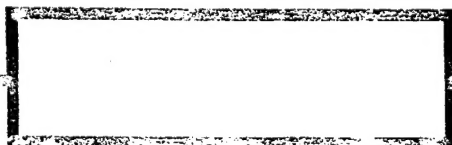Li Zhongya, Deng He, Fan Zhengxiu

DTIC QUALITY INSPECTED 5

19950512 071

I

HUMAN TRANSLATION

NAIC-ID(RS)T-0647-93   14 April 1995

MICROFICHE NR: 95C000213

1.06 μm LASER-INDUCED DAMAGE OF TI AND ZR THIN-FILM
OPTICAL COATINGS

By: Li Zhongya, Deng He, Fan Zhengxiu

English pages: 12

Source: Zhongguo Jiguang, Vol. 16, Nr. 7, July 1989;
         pp. 413-416

Country of origin: China
Translated by: SCITRAN
                F33657-84-D-0165
Requester: NAIC/TATD/Bruce Armstrong
Approved for public release; Distribution unlimited.

GRAPHICS DISCLAIMER

All figures, graphics, tables, equations, etc. merged into this
translation were extracted from the best quality copy available.

1.06 μm LASER-INDUCED DAMAGE OF TI AND ZR THIN-FILM OPTICAL COATINGS[1]

Li Zhongya   Deng He   Fan Zhengxiu

ABSTRACT

This article reports on 1.06 μm laser damage threshold values and damage appearance on TiO_2 and ZrO_2 as well as Ti_3O_5 single layer films and multilayer films. It studies the relationships between damage threshold values and film thickness, defects and protective coatings.

KEY WORDS   Damage, Optical Thin Films, Defect

I.   INTRODUCTION

Laser damage to optical thin films limits further increases in laser power levels. In recent years—both domestically and abroad—research on optical thin film laser damage has already achieved relatively great progress [1-4]. However, such problems as the physical processes associated with laser and thin film interactions as well as damage mechanisms and so on still await the carrying out of in depth research.

This article reports on laser damage threshold values and damage appearance in single layer films and multilayer films for different thicknesses of the three types of material—ZrO_2, TiO_2, and Ti_3O_5. It studies the relationship of film thickness and defects to damage threshold values, the influences of technical conditions on damage threshold values, and the action of protective films.

II. EXPERIMENTAL EQUIPMENT AND METHODS

2.1 Experimental Equipment

Equipment to carry out optical thin film laser damage experiments was as shown in Fig.1. Laser systems were composed of one stage oscillation and two stage amplification YAG lasers. As far as oscillators are concerned, option was made for the use of $LiF:F_2^{-1}$ crystal Q modulation and small aperture diaphragm mode selection. Output wave length was 1.06 μm, TEMOO mode, facula radius 44 μm. Pulse width was 10ns. Oscillator output laser beams go through amplification. They converge on sample films through an anti-image error nonspherical lens (f=80.4mm). Samples were placed on a three dimension moveable precision adjustment rack. During experiments, this was not only capable of conveniently moving samples. At the same time, it was also possible to make use of this system--using knife edge scanning methods--to accurately measure focal striation surface areas. He-Ne lasers were adjusted coaxial with main laser beams, using them in order to adjust the entire optical system. Microscopes were used in order to carry out detailed observations and diagnoses of sample damage.
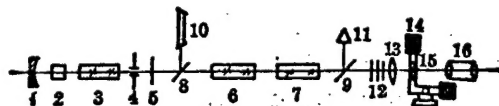
2.2 Damage Threshold Valuation

Fig.1 Experimental Equipment Schematic
Key: 1--R=3m Full Reflection Mirror 2--LiF Crystal 3--YAG Oscillator Rod 4--Small Aperture Diaphragm 5--Output Cavity Lens T=50% 6 and 7--YAG Amplifier Rods 8 and 9--Beam Splitting Mirrors 10--He-Ne Laser 11--Energy Meter 12--Light Filters 13--Nonspherical Lens 14--Sample Rack 15--Sample 16--Microscope

Valuation of measured damage threshold values is as follows:

$$E_{th} = \frac{\frac{1}{2}[E_{max}(ND) + E_{min}(D)]}{A} \tag{1}$$

In the equation, $E_{max}(ND)$ is the highest energy which does not give rise to coating damage. $E_{min}(D)$ is the lowest energy which does give rise to coating damage. A is the facula area associated with $1/e^2$ where strength on the coating is greater than center light strength.

The expansion range defining loss threshold values is

$$S = \frac{E_{max}(ND) - E_{min}(D)}{\frac{1}{2}[E_{max}(ND) + E_{min}(D)]} \tag{2}$$

S often acts as the criterion for measuring semiquantitative damage process statistical properties.

Damage experiments opt for the use of 1-on-1 methods of execution, that is, at one location on samples, there is only one iteration of laser light irradiation regardless of whether or not this point is damaged. Thin film sample typical laser damage follows energy distributions as shown in Fig.2. In the Fig.

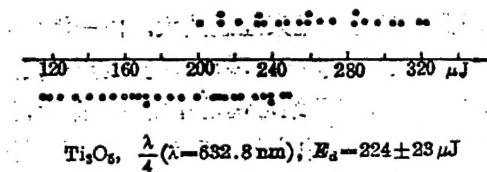$$E_d = \frac{1}{2}[E_{max}(ND) + E_{min}(D)] \pm \frac{S}{2}.$$

Ti_3O_5, $\frac{\lambda}{4}(\lambda = 632.8\,nm)$; $E_d = 224 \pm 23\,\mu J$

Fig.2 Laser Damage Distribution   *--damage   O--no damage

III. EXPERIMENTAL RESULTS AND DISCUSSION

3.1 Relationship Between Damage Threshold Values and Film Thickness

Newnam reported that relationships between TiO_2 damage threshold values and film thickness originated in different film interior field strength distributions [5]. When damage threshold value data is corrected for interior field strengths, it seems to support Newnam's conclusion. However, in reference [1], after corrections were made for interior fields in the majority of experimental data associated with films of different materials, there still existed relationships between damage threshold values and film thickness. However, Walker and others thought that, in the case of ZrO_2, HfO_2, and TiO_2, basically, relationships between destruction threshold values and film thicknesses do not exist. Their conclusion is that relationships between damage threshold values and film thicknesses are not capable of being completely explained by the use of internal electromagnetic fields.

We carried out laser damage experiments on the three types of materials--TiO_2, ZrO_2, and Ti_3O_5--with different thicknesses. The results were as shown in Table 1. As far as films of these three types of materials are concerned, their damage threshold values and film thicknesses all show obvious corresponding relationships. All $\lambda/4$ thickness films had damage threshold values higher than $\lambda/2$ films by approximately one fold.

4

TABLE 1. DAMAGE THRESHOLD VALUE AND FILM THICKNESS RELATIONSHIPS

材 料 (1)	膜 厚 (2) ($\lambda=1.06\mu m$)	损伤阈值 (3) (J/cm^2)	扩 展 (4)
ZrO$_2$	$\frac{\lambda}{4}$	37.3±5.3	±14%
	$\frac{\lambda}{2}$	15.3±2.6	±17%
TiO$_2$	$\frac{\lambda}{4}$	31.7±5.7	±18%
	$\frac{\lambda}{2}$	17.6±2.6	±14%
Ti$_2$O$_5$	$\frac{\lambda}{4}$	21.9±3.3	±15%
	$\frac{\lambda}{2}$	11.4±1.8	±16%

Key: (1) Material (2) Film Thickness (3) Damage Threshold
Value (4) Expansion

Mechanism problems associated with the relationships between
damage threshold values and film thicknesses are relatively
complicated. Besides the action of interior electromagnetic
fields brought up above, the factors associated with defects and
impurities are capable of being more important. With regard to
pulses with pulse width 0 ~ 10ns, the most important damage
mechanism is the absorption of submicron diameter impurities. In
thin film situations, due to impurity sizes being limited by film
thicknesses, when thin film thicknesses decrease--due to the
corresponding part of impurity dimensions which can most easily
produce damage being eliminated--the result is that damage
probability decreases and damage threshold values go up. When
thin film thickness increases, defects and impurities
correspondingly increase. At the same time, film light
absorption and internal stresses also increase. Because of this,
thick films relatively easily produce damage. Therefore, most
film damage threshold values follow increases in thickness and go
down.

3.2 Protective Films Raise Polarization Film Damage Threshold Values

The main film system structures and technical conditions associated with polarization films 6-1 and 6-29 are basically the same. Sample 6-1 adds a $\lambda/2$ SiO_2 protective film (λ = 1.06 μm). Damage threshold value is 54.7 J/cm^2. Sample 6-29 does not add a protective film. The damage threshold value is 15.8 J/cm^2. Damage threshold values associated with samples having protective films were 2.5 times higher than those without protective films.

From thin film structure analysis [6], it is known that SiO_2 film is an amorphous structure. It displays a homogeneous granular state. Particle dimensions are approximately 25nm. SiO_2 film stress is relatively small. Film absorption is small. Because of this, it possesses the special characteristic of a strong capability to endure laser damage. As far as ordinary polarization films are concerned, the outermost layer is TiO_2 or ZrO_2. They are crystallization type structures. Put under tensile stress, they are easily destroyed. On polarization films, after adding a layer of SiO_2, film surface structure is improved. Because of this, polarization film laser damage threshold values very greatly increase.

3.3 Influence of Film Making Technology on Laser Damage Threshold Values

We carried out experiments on a group of Ti_3O_5 single layer film samples associated with a film thickness of $\lambda/4$ (λ = 632.8nm). First of all, in a GFS high reflection device, thin film transmission rates and reflection rates at 1.06 μm wavelength were measured. Calculations were done of thin film optical losses (including absorption and scattering losses, etc). Results are seen in Table 2. In particular, the influence of

6

insufficient oxygen on damage threshold values is very severe.
Comparing samples A and B, A does not have sufficient oxygen.
B does have sufficient oxygen. Other technical conditions are all
the same. A optical losses are 25 times higher than B. However,
damage threshold value A is approximately only 1/12th B. The
reason is because samples, during film plating processes, did not
have sufficient oxygen. Ti_3O_5 did not sufficiently oxidize to
become TiO_2. Electron microscope analysis results clearly show
that, in film layers, relatively abundant Ti_3O_5 is included. Due
to strong absorption associated with Ti_3O_5, sample A optical
losses are made particularly large. The damage threshold values
are several tens of times lower than ordinary samples. With
regard to samples C and D, because drying temperatures are not
the same, and other technical conditions are all the same, then,
their optical losses will also show doubling differences.
Table 2 results clearly show that film manufacturing techniques
have very large influences on film optical losses and damage
threshold values. Moreover, damage threshold values follow
increases in optical losses and go down.

3.4 Relationship Between Defect Density and Damage Threshold Values

Thin film defect distributions are usually random and
nonuniform. Because of this, it is very difficult to make
precise qualitative calculations of flaw densities. Domestically
and abroad, research on this problem is still scarce [7]. We
used the method below to determine thin film defect densities.
On samples, one location was selected randomly. Using Nomarski
microscopes, optical microscopic photographs magnified 700 times
were taken. Defects were clearly recorded in the photos.
Following this, calculations were done of defect densities d
(defect number/mm^2). In the case of 4 pieces of ZrO_2 single
layer film with a thickness of $\lambda/2$ (λ = 1.06 μm),
damage tests were carried out. The results were as shown in

7

Fig.3. Damage threshold values and the inverse of defect densities form direct proportions. Following reductions in defect densities, damage threshold value linearity increases. In experiments, it was discovered that, as far as samples with numerous defects are concerned, the damage threshold value expansion ranges were relatively broad--approximately 30 ~ 40%. However, with regard to samples with relatively good film layer quality, the expansion range is generally around 15%.

TABLE 2. INFLUENCES OF TECHNICAL CONDITIONS ON DAMAGE THRESHOLD VALUES

1 样品	2 工艺条件	3 光 损 耗	损伤阈值 4 (J/cm²)
A	5基板，300°C 烘烤 3 h，不 充 O₂	1.75×10^{-1}	0.51 ± 0.18
B	6基板，300°C 烘烤 3 h，充 O₂	6.8×10^{-3}	9.9 ± 1.1
C	7基板，250°C 烘烤 2 h，充 O₂	4.2×10^{-3}	14.7 ± 1.5
D	8基板，200°C 烘烤 2 h，充 O₂	2.2×10^{-3}	15.3 ± 2.1

Key: (1) Sample (2) Technical Conditions   (3) Optical Losses (4) Damage Threshold Value (5) Substrate, 300°C Drying 3h, Insufficient O_2 (6) Substrate, 300°C Drying 3h, Sufficient O_2 (7) Substrate, 250°C Drying 2h, Sufficient O_2 (8) Substrate, 200°C Drying 2h, Sufficient O_2
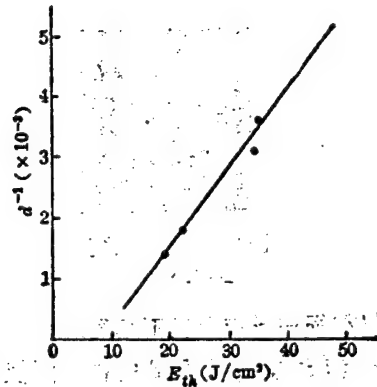
Fig.3 Relationship Between Damage Threshold Values and Defect Densities

3.5 Damage Appearance

Fig.4 is ZrO_2 film damage appearances for thicknesses $\lambda/2$ and $\lambda/4$. As far as Fig.4(a) and 4(b) are concerned, the materials and the thicknesses of the two samples are both the same. However, the appearances of their damage are very different. Sample 7-3 damage appearance is a peeled layer type. Damage spots are relatively large. Outside perimeters of spots are extremely irregular. In Fig.3, the damages associated with the 4 pieces of sample are all this type. The centers of sample 4 damage spots have a large number of small pits of unequal size. This type of sample was made into 2 pieces, and the damage appearances for both were like this. This is an ablative type. These two types of film are not only very different. Moreover, damage threshold values also differ from each other relatively greatly. Sample 7-3 damage threshold values are higher than Sample 4 by more than 40%. The reason is, we believe, primarily that technical conditions are different.

9

These two types of film were made on two different film plating units. Sample 7-3 drying temperature was 150°C for 2 hours, oxygen supply $1x10^{-4}$ Torr. Sample 4 drying temperature was 250°C for 2.5 hours, oxygen supply $2x10^{-4}$ Torr. It is possible to see that work techniques have very great influences on both film damage threshold values and appearance. Because of this, strict control of technical conditions associated with film manufacture has very important significance for improving ZrO_2 film quality and raising antilaser damage levels.
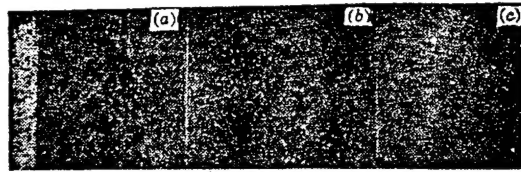
/416

Fig.4 ZrO_2 Film

(a)   7-3, $\lambda/2$, 1000x;   (b)   4, $\lambda/2$, 3200x;   (c)   2, $\lambda/4$, 2800x
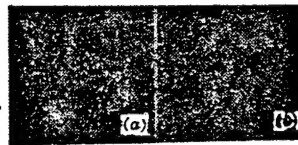

Fig.5

TiO_2 Film   (a)   5, $\lambda/2$, 2000x;   (b)   6, $\lambda/4$, 2400x
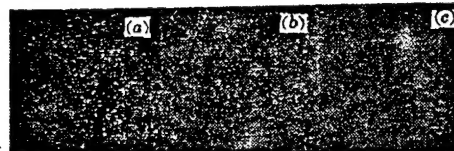

Fig.6 Ti_3O_5 Film

(a)   11, $\lambda/2$, 2000X;   (b)   11, $\lambda/2$, 1700X;   (c)   9, $\lambda/4$, 1500X
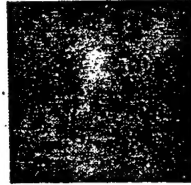
10

Fig.7   Semitransmissive Semireflective Film

24-1, 850X

Fig.4(c) is the damage appearance associated with ZrO_2 film of thickness $\lambda/4$. Spots are relatively small. It presents a picture of uniform ablative damage.

(2)   Fig.5 is damage appearances associated with different thicknesses of TiO_2. The appearances in Fig.5(a) and (b) are basically the same, showing one-area-at-a-time ablative damage. When laser energy acting on film surfaces is one fold or more higher than damage threshold values, outside rings of spots show the appearance of atomization phenomena.

(3)   Fig.6 is damage appearances associated with different thicknesses of Ti_3O_5 film. Laser energies associated with Fig.6(a) and (c) are slightly higher than threshold damage values. Damage spots are an ablative type. The laser energy associated with Fig.6(b) is roughly two fold higher than damage threshold values. Spots show clearly fused states.

(4)   Fig.7 is a three layer TiO_2/SiO_2 semitransmissive semireflective film. The outermost layer adds a $\lambda/2$ SiO_2 protective film. The centers of damage spots are fused. The

11

outermost surface layer SiO_2 film shows a ruptured condition. Above, it has already been brought out that, because SiO_2 absorptions are small, it possesses a characteristically strong capability to withstand laser destruction. When interior TiO_2 films sustain laser light irradiation fusing, they produce very large shock forces, causing SiO_2 film to rupture. For this reason, one gets the production of irregular surface rupture and destruction.

As far as all films--in the process of carrying out damage tests--are concerned, when film layers give rise to destruction, in all cases, it is accompanied by the appearance of a light blue colored plasma flash.

REFERENCES

1   T. W. Walker *et al.*, *IEEE J. Quant. Electr.*, QE-17(10), 2041(1981)
2   W. H. Lowdermilk, D. Milam, *IEEE J. Quant. Electr.*, QE-17(9), 1888(1981)
3   K. H. Guenther *et al.*, *Appl. Opt.*, 23(21), 3743 (1984)
4   F. Rainer *et al.*, *Appl. Opt.*, 24(4), 496(1985)
5   B. E. Newnam *et al.*, (NBS Special Publication 435, 1975), 254
6   上海光机所研究报告集，第三集，1976, p. 146
7   M. E. Innocenzi *et al.*, *Appl. Opt.*, 25(5), 653 (1986)

DISTRIBUTION LIST

DISTRIBUTION DIRECT TO RECIPIENT

ORGANIZATION	MICROFICHE
BO85 DIA/RTS-2FI	1
C509 BALLOC509 BALLISTIC RES LAB	1
C510 R&T LABS/AVEADCOM	1
C513 ARRADCOM	1
C535 AVRADCOM/TSARCOM	1
C539 TRASANA	1
Q592 FSTC	4
Q619 MSIC REDSTONE	1
Q008 NTIC	1
Q043 AFMIC-IS	1
E051 HQ USAF/INET	1
E404 AEDC/DOF	1
E408 AFWL	1
E410 AFDTC/IN	1
E429 SD/IND	1
P005 DOE/ISA/DDI	1
P050 CIA/OCR/ADD/SD	2
1051 AFIT/LDE	1
PO90 NSA/CDB	1
2206 FSL	1

Microfiche Nbr: FTD95C000213

NAIC-ID(RS)T-647-93